

Copolymers Near a Linear Selective Interface

A *copolymer* is a polymer consisting of different types of monomer. In this chapter we consider a two-dimensional *directed* copolymer, consisting of a random concatenation of *hydrophobic* and *hydrophilic* monomers, near a linear interface separating two immiscible solvents, *oil* and *water* (see Fig. 9.1). We will be interested in the *quenched* path measure (of the type defined in (1.3)). We will show that, as a function of the strength and the bias of the interaction between the monomers and the solvents, this model has a phase transition between a *localized* phase, where the copolymer stays near the interface, and a *delocalized* phase, where the copolymer wanders away from the interface. The critical curve separating the two phases has interesting properties, some of which remain to be clarified. The main techniques used are the *subadditive ergodic theorem*, the *method of excursions*, *large deviations* and *partial annealing estimates*.

In Section 9.1 we define the model, in Section 9.2 we study the free energy, in Section 9.3 we prove the existence of the phase transition, in Section 9.4 we identify the qualitative properties of the critical curve, while in Section 9.5 we describe the qualitative properties of the two phases.

In Chapter 10 we will turn to a model where the linear interface is replaced by a random interface, coming from large blocks of oil and water arranged in a percolation-type fashion.

The order of the monomers is determined by the *polymerization process* through which the copolymer is grown (see Section 1.1). Since the monomers cannot reconfigure themselves without some chemical reaction occurring, a copolymer is an example of a system with *quenched* disorder. Different copolymers typically have different orderings of monomers. Therefore, in order to determine the physical properties of a system of copolymers, an average must be taken over the possible monomer orderings. This is why it is natural to consider the monomers as being drawn *randomly* according to some appropriate probability distribution, i.i.d. in our case.

Copolymers near liquid-liquid interfaces are of interest due to their extensive application as surfactants, emulsifiers, and foaming or antifoaming agents.

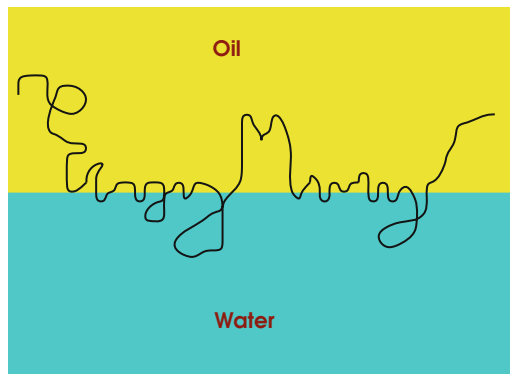


Fig. 9.1. An undirected copolymer near a linear interface.

Many fats contain stretches of hydrophobic and hydrophilic monomers, arranged “in some sort of erratic manner”, and therefore are examples of random copolymers. The transition between a localized and a delocalized phase has been observed experimentally e.g. in neutron reflection studies of copolymers consisting of blocks of ethylene oxide and propylene oxide near a hexane-water interface (Phipps, Richardson, Cosgrove and Eaglesham [266]). Here, a thin layer of hexane, approximately 10^{-5} m thick, is spread on water. In the localized phase, the copolymer is found to stretch itself along the interface in a band of width approximately 20 \AA .

Soteros and Whittington [283], Sections 2.2, 3.2.2 and 4.2.2, describes a number of rigorous, approximate, numerical and heuristic results for copolymers near linear interfaces. An earlier reference is Whittington [316]. Giacomini [116], Chapters 6–9, gives an overview of rigorous and numerical results based on the method of excursions.

9.1 A Copolymer Interacting with Two Solvents

For $n \in \mathbb{N}_0$, let

$$\mathcal{W}_n = \{w = (i, w_i)_{i=0}^n : w_0 = 0, w_{i+1} - w_i = \pm 1 \ \forall 0 \leq i < n\} \quad (9.1)$$

denote the set of all n -step directed paths in $\mathbb{N}_0 \times \mathbb{Z}$ that start from the origin and at each step move either north-east or south-east (called ballot paths; recall Fig. 1.4). This is the set of configurations of the copolymer. An example of a path in \mathcal{W}_n is drawn in Fig. 9.2. Let

$$\omega = (\omega_i)_{i \in \mathbb{N}} \text{ be i.i.d. with } \mathbb{P}(\omega_1 = +1) = \mathbb{P}(\omega_1 = -1) = \frac{1}{2}. \quad (9.2)$$

This random sequence labels the order of the monomers along the copolymer (see Fig. 9.2). Throughout the sequel, \mathbb{P} denotes the law of ω . As Hamiltonian we pick, for fixed ω ,

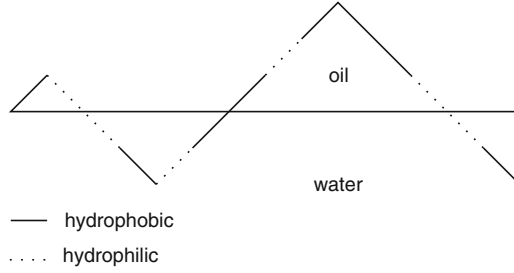


Fig. 9.2. A 14-step directed copolymer near a linear interface. Oil is above the interface, water is below. The drawn edges are hydrophobic monomers, the dashed edges are hydrophilic monomers.

$$H_n^\omega(w) = -\lambda \sum_{i=1}^n (\omega_i + h) \text{sign}(w_{i-1}, w_i), \quad w \in \mathcal{W}_n, \quad (9.3)$$

with $\text{sign}(w_{i-1}, w_i) = \pm 1$ depending on whether the edge (w_{i-1}, w_i) lies above or below the horizontal axis, and $\lambda, h \in \mathbb{R}$. Without loss of generality we may restrict the interaction parameters to the quadrant

$$\text{QUA} = \{(\lambda, h) \in [0, \infty)^2\}. \quad (9.4)$$

The choice in (9.3) has the following interpretation. Think of $w \in \mathcal{W}_n$ as a directed copolymer on $\mathbb{N}_0 \times \mathbb{Z}$, consisting of n monomers represented by the edges in the path (rather than the sites). The lower halfplane is water, the upper halfplane is oil. The monomers are labeled by ω , with $\omega_i = +1$ meaning that monomer i is hydrophobic and $\omega_i = -1$ that it is hydrophilic. The term $\text{sign}(w_{i-1}, w_i)$ equals $+1$ or -1 depending on whether monomer i lies in the oil or in the water. Thus, the Hamiltonian rewards matches and penalizes mismatches of the chemical affinities between the monomers and the solvents. The parameter λ is the *disorder strength*. The parameter h plays the role of an *disorder bias*: $h = 0$ corresponds to the hydrophobic and hydrophilic monomers interacting equally strongly, while $h = 1$ corresponds to the hydrophilic monomers not interacting at all. Only the regime $h \in [0, 1]$ is of interest (because for $h > 1$ both types of monomers prefer to be in the oil and the copolymer is always delocalized).

The law of the copolymer given ω is denoted by P_n^ω and is defined as in (1.3), i.e.,

$$P_n^\omega(w) = \frac{1}{Z_n^\omega} e^{-H_n^\omega(w)} P_n(w), \quad w \in \mathcal{W}_n, \quad (9.5)$$

where P_n is the law of the n -step directed random walk, which is the uniform distribution on \mathcal{W}_n . This law is the projection on \mathcal{W}_n of the law P of the infinite directed walk whose vertical steps are SRW. Note that we have suppressed λ, h from the notation.

In what follows we will consider the *quenched free energy* $f(\lambda, h)$ of the copolymer, i.e., the free energy conditioned on ω . We will first show that $f(\lambda, h)$ exists and is constant ω -a.s. We will then show that $f(\lambda, h)$ is non-analytic along a *critical curve* in the (λ, h) -plane, derive a number of properties of this curve, and subsequently have a look at the typical behavior of the copolymer in each of the two phases.

The model defined in (9.3) was introduced in Garel, Huse, Leibler and Orland [111], where the existence of a phase transition was argued on the basis of non-rigorous arguments. The first rigorous studies were carried out in Sinai [274] and in Bolthausen and den Hollander [31]. The latter paper proved the existence of a phase transition, derived a number of properties of the critical curve, and raised a number of questions. Since then, several papers have appeared in which these questions have been settled and various aspects of the model have been further elucidated, leading not only to many interesting results, but also to challenging open problems. We will refer to these papers as we go along.

In Giacomin [116], Chapters 6–9, the more general situation is considered where the ω_i are \mathbb{R} -valued with a finite moment generating function and the $w_{i+1} - w_i$ are the increments of a random walk in the domain of attraction of a stable law. We will comment on this extension in Section 9.6. The special situation treated below (SRW and binary disorder) already collects the main ideas.

A key observation is the following. The energy of a path is a sum of contributions coming from its *successive excursions* away from the interface (see Fig. 9.2). What is relevant for the energy of these excursions is when they start and end, and whether they are above or below the interface. This simplifying feature, together with the directed nature of the path, is of great help when we want to do explicit calculations.

9.2 The Free Energy

Our starting point is the following self-averaging property, which is taken from Bolthausen and den Hollander [31].

Theorem 9.1. *For every $\lambda, h \in \text{QUA}$,*

$$f(\lambda, h) = \lim_{n \rightarrow \infty} \frac{1}{n} \log Z_n^\omega \quad (9.6)$$

exists ω -a.s. and in \mathbb{P} -mean, and is constant ω -a.s.

Proof. The proof consists of two parts. In Lemma 9.2 we prove that the claim holds when the random walk is constrained to return to the origin at time $2n$. In Lemma 9.3 we show how to remove this constraint.

Fix $\lambda, h \in \text{QUA}$. Abbreviate

$$\Delta_i = \text{sign}(S_{i-1}, S_i) \quad (9.7)$$

and define

$$Z_{2n}^{\omega,0} = E \left(\exp \left[\lambda \sum_{i=1}^{2n} (\omega_i + h) \Delta_i \right] 1_{\{S_{2n}=0\}} \right), \quad (9.8)$$

where we recall that P is the law of SRW, $S = (S_i)_{i \in \mathbb{N}_0}$.

Lemma 9.2. $\lim_{n \rightarrow \infty} \frac{1}{2n} \log Z_{2n}^{\omega,0}$ exists ω -a.s. and in \mathbb{P} -mean, and is constant ω -a.s.

Proof. We need the following three properties:

- (I) $Z_{2n}^{\omega,0} \geq Z_{2m}^{\omega,0} Z_{2n-2m}^{T^{2m}\omega,0}$ for all $0 \leq m \leq n$, with T the left-shift acting on ω as $(T\omega)_i = \omega_{i+1}$, $i \in \mathbb{N}$.
- (II) $n \rightarrow \frac{1}{2n} \mathbb{E}(\log Z_{2n}^{\omega,0})$ is bounded from above.
- (III) $\mathbb{P}(T\omega \in \cdot) = \mathbb{P}(\omega \in \cdot)$.

Property (I) follows from (9.8) by inserting an extra indicator $1_{\{S_{2m}=0\}}$ and using the Markov property of S at time $2m$. Property (II) holds because

$$\begin{aligned} \mathbb{E} \left(\log Z_{2n}^{\omega,0} \right) &\leq \log \mathbb{E} \left(Z_{2n}^{\omega,0} \right) \\ &= \log E \left((\cosh \lambda)^{2n} \exp \left[\lambda h \sum_{i=1}^{2n} \Delta_i \right] 1_{\{S_{2n}=0\}} \right) \\ &\leq 2n(\log \cosh \lambda + \lambda h). \end{aligned} \quad (9.9)$$

Property (III) is trivial. Thus, $\omega \mapsto (\log Z_{2n}^{\omega,0})_{n \in \mathbb{N}_0}$ is a *superadditive random process* (which is the analogue of a superadditive deterministic sequence mentioned in Section 1.3). It therefore follows from the *subadditive ergodic theorem* (Kingman [214]) that $\lim_{n \rightarrow \infty} \frac{1}{2n} \log Z_{2n}^{\omega,0}$ converges ω -a.s. and in \mathbb{P} -mean, and is measurable w.r.t. the tail sigma-field of ω . Since the latter is trivial, i.e., all events not depending on finitely many coordinates have probability 0 or 1, the limit is constant ω -a.s. \square

Our original partition sum at time $2n$ was

$$Z_{2n}^{\omega} = E \left(\exp \left[\lambda \sum_{i=1}^{2n} (\omega_i + h) \Delta_i \right] \right), \quad (9.10)$$

which is (9.8) but without the indicator. Thus, in order to prove Theorem 9.1 we must show that this indicator is harmless as $n \rightarrow \infty$. Since $|\log(Z_{2n}^{\omega}/Z_{2n+1}^{\omega})| \leq \lambda(1+h)$, it will suffice to consider time $2n$.

Lemma 9.3. *There exists a $C < \infty$ such that $Z_{2n}^{\omega,0} \leq Z_{2n}^{\omega} \leq Cn Z_{2n}^{\omega,0}$ for all $n \in \mathbb{N}$ and ω .*

Proof. The lower bound is obvious. The upper bound is proved as follows (compare with the proof of Theorem 7.1). For $1 \leq k \leq n$, consider the events

$$\begin{aligned} A_{2n,2k}^+ &= \{S_i > 0 \text{ for } 2n - 2k + 1 \leq i \leq 2n\}, \\ B_{2n,2k}^+ &= \{S_i > 0 \text{ for } 2n - 2k + 1 \leq i < 2n, S_{2n} = 0\}, \end{aligned} \quad (9.11)$$

and similarly for $A_{2n,2k}^-, B_{2n,2k}^-$ when the excursion is below the interface. By conditioning on the last hitting time of 0 prior to time $2n$, we may write

$$\begin{aligned} Z_{2n}^\omega &= Z_{2n}^{\omega,0} + \sum_{k=1}^n Z_{2n-2k}^{\omega,0} E \left(\exp \left[\lambda \sum_{i=2n-2k+1}^{2n} (\omega_i + h) \Delta_i \right] \right. \\ &\quad \left. \times 1\{A_{2n,2k}^+ \cup A_{2n,2k}^-\} \mid S_{2n-2k} = 0 \right) \\ &= Z_{2n}^{\omega,0} + \sum_{k=1}^n Z_{2n-2k}^{\omega,0} \frac{a(2k)}{b(2k)} E \left(\exp \left[\lambda \sum_{i=2n-2k+1}^{2n} (\omega_i + h) \Delta_i \right] \right. \\ &\quad \left. \times 1\{B_{2n,2k}^+ \cup B_{2n,2k}^-\} \mid S_{2n-2k} = 0 \right). \end{aligned} \quad (9.12)$$

The reason for the second equality in (9.12) is that $\Delta_i = +1$ for all $2n - 2k + 1 \leq i \leq 2n$ on the events $A_{2n,2k}^+, B_{2n,2k}^+$ and $\Delta_i = -1$ for all $2n - 2k + 1 \leq i \leq 2n$ on the events $A_{2n,2k}^-, B_{2n,2k}^-$ (ω is fixed). We have

$$\begin{aligned} P(A_{2n,2k}^+ \mid S_{2n-2k} = 0) &= P(A_{n,k}^- \mid S_{2n-2k} = 0) = a(2k), \\ P(B_{2n,2k}^+ \mid S_{2n-2k} = 0) &= P(B_{n,k}^- \mid S_{2n-2k} = 0) = b(2k), \end{aligned} \quad (9.13)$$

where (compare with (7.4))

$$\begin{aligned} a(2k) &= P(S_i > 0 \text{ for } 1 \leq i \leq 2k \mid S_0 = 0), \\ b(2k) &= P(S_i > 0 \text{ for } 1 \leq i < 2k, S_{2k} = 0 \mid S_0 = 0). \end{aligned} \quad (9.14)$$

Moreover, there exist $0 < C_1, C_2 < \infty$ such that $a(2k) \sim C_1/k^{1/2}$ and $b(2k) \sim C_2/k^{3/2}$ as $k \rightarrow \infty$ (see Spitzer [284], Section 1). Hence $a(2k)/b(2k) \leq Ck$, $k \in \mathbb{N}$, for some $C < \infty$. Finally, without the factor $a(2k)/b(2k)$ the last sum in (9.12) is precisely $Z_{2n}^{\omega,0}$. Hence we get

$$Z_{2n}^\omega \leq (1 + Cn) Z_{2n}^{\omega,0}, \quad (9.15)$$

which proves the claim. \square

Lemmas 9.2–9.3 complete the proof of Theorem 9.1. \square

9.3 The Critical Curve

Now that we have proved the existence of the quenched free energy, we proceed to study its properties, in particular, we proceed to look for a phase transition in QUA. In Section 9.3.1 we define the localized and the delocalized phases, while in Section 9.3.2 we prove the existence of a non-trivial critical curve separating the two. Sections 9.4–9.5 will be devoted to establishing the qualitative properties of the critical curve and the two phases.

Grosberg, Izrailev and Nechaev [133] and Sinai and Spohn [276] study the annealed version of the model, in which Z_n^ω is averaged over ω . The free energy and the critical curve can in this case be computed exactly, but they provide little information on what the quenched model does. Nevertheless, in Section 9.4.1 we will use the annealed model to obtain an upper bound on the quenched critical curve.

9.3.1 The Localized and Delocalized Phases

The quenched free energy $f(\lambda, h)$ is continuous, nondecreasing and convex in each variable (convexity follows from Hölder's inequality, as shown in Section 1.3). Moreover, we have

$$f(\lambda, h) \geq \lambda h \quad \forall (\lambda, h) \in \text{QUA}. \quad (9.16)$$

Indeed, since $P(\Delta_i = +1 \forall 1 \leq i \leq n) \sim C/n^{1/2}$ for some $C > 0$ as $n \rightarrow \infty$ (see Spitzer [284], Section 7), it follows from (9.3–9.5) that

$$\begin{aligned} Z_n^\omega &= E \left(\exp \left[\lambda \sum_{i=1}^n (\omega_i + h) \Delta_i \right] \right) \\ &\geq \left(\exp \left[\lambda \sum_{i=1}^n (\omega_i + h) \Delta_i \right] 1_{\{\Delta_i = +1 \forall 1 \leq i \leq n\}} \right) \\ &= \exp \left[\lambda \sum_{i=1}^n (\omega_i + h) \right] P(\Delta_i = +1 \forall 1 \leq i \leq n) \\ &= \exp[\lambda h n + o(n) = O(\log n)] \quad \omega - a.s., \end{aligned} \quad (9.17)$$

where in the last line we use the strong law of large numbers for ω . Thus, we see that the lower bound in (9.16) corresponds to the strategy where the copolymer wanders away from the interface in the upward direction. This leads us to the following definition (see Fig. 9.3).

Definition 9.4. *We say that the copolymer is:*

- (i) *localized if $f(\lambda, h) > \lambda h$,*
- (ii) *delocalized if $f(\lambda, h) = \lambda h$.*

We write

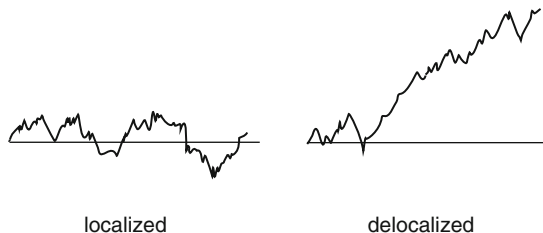


Fig. 9.3. Expected path behavior in the two phases.

$$\begin{aligned}\mathcal{L} &= \{(\lambda, h) \in \text{QUA} : f(\lambda, h) > \lambda h\}, \\ \mathcal{D} &= \{(\lambda, h) \in \text{QUA} : f(\lambda, h) = \lambda h\},\end{aligned}\tag{9.18}$$

to denote the localized, respectively, the delocalized region in QUA.

In case (i), the copolymer is able to beat on an exponential scale the trivial strategy of moving upward. It is intuitively clear that this is only possible by crossing the interface at a positive frequency, but a proof of the latter requires work. In case (ii), the copolymer is not able to beat the trivial strategy on an exponential scale. In principle it could do better on a smaller scale, but it actually does not, which also requires work. Path properties are dealt with in Section 9.5.1.

Albeverio and Zhou [1] prove that if $\lambda > 0$ and $h = 0$, then $\log Z_n^\omega$ satisfies a law of large numbers and a central limit theorem (as a random variable in ω). This result readily extends to the entire localization regime.

9.3.2 Existence of a Non-trivial Critical Curve

The following theorem, taken from Bolthausen and den Hollander [31], shows that \mathcal{L} and \mathcal{D} are separated by a non-trivial critical curve (see Fig. 9.4).

Theorem 9.5. *For every $\lambda \in [0, \infty)$ there exists an $h_c(\lambda) \in [0, 1)$ such that the copolymer is*

$$\begin{array}{ll} \text{localized} & \text{if } 0 \leq h < h_c(\lambda), \\ \text{delocalized} & \text{if } h \geq h_c(\lambda). \end{array}\tag{9.19}$$

Moreover, $\lambda \mapsto h_c(\lambda)$ is continuous and strictly increasing on $[0, \infty)$, with $h_c(0) = 0$ and $\lim_{\lambda \rightarrow \infty} h_c(\lambda) = 1$.

Proof. Let

$$g_n^\omega(\lambda, h) = \frac{1}{n} \log E \left(\exp \left[\lambda \sum_{i=1}^n (\omega_i + h)(\Delta_i - 1) \right] \right). \tag{9.20}$$

Then, because $\lambda \sum_{i=1}^n (\omega_i + h) = \lambda h + o(n)$ ω -a.s., Theorem 9.1 says that

$$\lim_{n \rightarrow \infty} g_n^\omega(\lambda, h) = g(\lambda, h) \quad \omega - a.s. \tag{9.21}$$

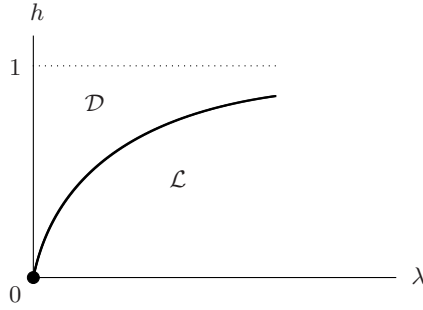


Fig. 9.4. Plot of $\lambda \mapsto h_c(\lambda)$.

with

$$g(\lambda, h) = f(\lambda, h) - \lambda h \quad (9.22)$$

the *excess free energy*. In terms of g , (9.18) becomes

$$\begin{aligned} \mathcal{L} &= \{(\lambda, h) \in \text{QUA} : g(\lambda, h) > 0\}, \\ \mathcal{D} &= \{(\lambda, h) \in \text{QUA} : g(\lambda, h) = 0\}. \end{aligned} \quad (9.23)$$

For $\lambda \in [0, \infty)$, define

$$h_c(\lambda) = \inf\{h \in [0, \infty) : (\lambda, h) \in \mathcal{D}\}. \quad (9.24)$$

To study this function, it is expedient to change variables by putting

$$\theta = \lambda h, \quad \theta_c(\lambda) = \lambda h_c(\lambda), \quad \bar{g}(\lambda, \theta) = g(\lambda, h). \quad (9.25)$$

Because λ and θ appear linearly in the Hamiltonian in (9.3), we know that $(\lambda, \theta) \mapsto \bar{g}(\lambda, \theta)$ is convex (see Section 1.3). Moreover, since $\bar{g} \geq 0$, we have $\mathcal{D} = \{(\lambda, \theta) : \bar{g}(\lambda, \theta) \leq 0\}$, i.e., \mathcal{D} is a level set of the function \bar{g} . Since \bar{g} is a convex function, it follows that \mathcal{D} is a convex set, implying in turn that \mathcal{L} and \mathcal{D} are separated by a *single* critical curve

$$\theta_c(\lambda) = \inf\{\theta \in [0, \infty) : (\lambda, \theta) \in \mathcal{D}\} \quad (9.26)$$

that is itself a convex function.

We know that $h_c(0) = 0$. Now, Theorems 9.6–9.7 below will imply that

$$0 < \liminf_{\lambda \downarrow 0} \frac{1}{\lambda} h_c(\lambda) \leq \limsup_{\lambda \downarrow 0} \frac{1}{\lambda} h_c(\lambda) < \infty. \quad (9.27)$$

Moreover, Theorem 9.7 will imply that $\lim_{\lambda \rightarrow \infty} h_c(\lambda) = 1$. All that therefore remains to be done is to show that h_c is strictly increasing on $[0, \infty)$. To that end, note that $\theta_c(0) = 0$, while (9.27) shows that $\theta_c(\lambda)$ is of order λ^2 near 0. Consequently, $\lambda \mapsto \theta_c(\lambda)/\lambda$ is strictly increasing $[0, \infty)$ (with limiting value 0 at $\lambda = 0$). \square

The critical curve in Fig. 9.4 shows that at high temperature (small λ) *entropic* effects dominate, causing the copolymer to wander away from the interface, while at low temperature (large λ) *energetic* effects dominate, causing the copolymer to stay close to the interface. The crossover value of λ depends on the value of h .

9.4 Qualitative Properties of the Critical Curve

In Section 9.4.1 we derive an upper bound on the critical curve, in Section 9.4.2 a lower bound, while in Section 9.4.3 we indicate that it has a (positive and finite) slope at 0.

9.4.1 Upper Bound

The next result, also taken from Bolthausen and den Hollander [31], provides an upper bound on h_c . This bound is the critical curve for the *annealed* model.

Theorem 9.6. $h_c(\lambda) \leq (2\lambda)^{-1} \log \cosh(2\lambda)$ for all $\lambda \in (0, \infty)$.

Proof. Estimate (recall (9.20–9.22))

$$\begin{aligned} g(\lambda, h) &= \lim_{n \rightarrow \infty} \frac{1}{n} \mathbb{E} \left(\log E \left(\exp \left[\lambda \sum_{i=1}^n (\omega_i + h)(\Delta_i - 1) \right] \right) \right) \\ &\leq \lim_{n \rightarrow \infty} \frac{1}{n} \log E \left(\mathbb{E} \left(\exp \left[\lambda \sum_{i=1}^n (\omega_i + h)(\Delta_i - 1) \right] \right) \right) \\ &= \lim_{n \rightarrow \infty} \frac{1}{n} \log E \left(\prod_{i=1}^n \left[\frac{1}{2} e^{-2\lambda(1+h)} + \frac{1}{2} e^{-2\lambda(-1+h)} \right]^{1_{\{\Delta_i = -1\}}} \right). \end{aligned} \quad (9.28)$$

The first equality comes from the fact that Kingman's subadditive ergodic theorem holds in \mathbb{P} -mean. The inequality follows from Jensen's inequality and Fubini's theorem. The second equality uses (9.2). The right-hand side is ≤ 0 as soon as the term between square brackets is ≤ 1 . Consequently,

$$(2\lambda)^{-1} \log \cosh(2\lambda) > h \implies g(\lambda, h) = 0, \quad (9.29)$$

which yields the desired upper bound on $h_c(\lambda)$. \square

Note that the proof of Theorem 9.6 is a *partial annealing estimate* in disguise, because to transform (9.18) into (9.23) we have used the law of large numbers for ω .

9.4.2 Lower Bound

The following counterpart of Theorem 9.6, due to Bodineau and Giacomin [22], provides a lower bound on $h_c(\lambda)$.

Theorem 9.7. $h_c(\lambda) \geq (\frac{4}{3}\lambda)^{-1} \log \cosh(\frac{4}{3}\lambda)$ for all $\lambda \in (0, \infty)$.

Proof. As we will see, the lower bound comes from strategies where the copolymer dips below the interface during rare long stretches in ω where the empirical mean is sufficiently biased.

We begin with some notation. Pick $l \in 2\mathbb{N}$. For $j \in \mathbb{N}$, let

$$I_j = ((j-1)l, jl] \cap \mathbb{N}, \quad \Omega_j = \sum_{i \in I_j} \omega_i. \quad (9.30)$$

Pick $\delta \in (0, 1]$. Define recursively

$$i_0^\omega = 0, \quad i_j^\omega = \inf\{k \geq i_{j-1}^\omega + 2: \Omega_k \leq -\delta l\}, \quad j \in \mathbb{N}, \quad (9.31)$$

and abbreviate $\tau_j^\omega = i_j^\omega - i_{j-1}^\omega - 1$, $j \in \mathbb{N}$. (In (9.31) we skip at least 2 to make sure that $\tau_j^\omega \geq 1$, which is needed below.) For $n \in \mathbb{N}$, put

$$t_{n,l,\delta}^\omega = \sup\{j \in \mathbb{N}: i_j^\omega \leq \lfloor n/l \rfloor\}, \quad (9.32)$$

and consider the set of paths (see Fig. 9.5)

$$\begin{aligned} \mathcal{W}_{n,l,\delta}^\omega = \Big\{ w \in \mathcal{W}_n: & \quad w_i \leq 0 \text{ for } i \in \bigcup_{j=1}^{t_{n,l,\delta}^\omega} I_{i_j^\omega}^\omega, \\ & \quad w_i \geq 0 \text{ for } i \in \{(0, n] \cap \mathbb{N}\} \setminus \bigcup_{j=1}^{t_{n,l,\delta}^\omega} I_{i_j^\omega}^\omega \Big\}. \end{aligned} \quad (9.33)$$

By restricting the path to $\mathcal{W}_{n,l,\delta}^\omega$, we find that the quantity in (9.20) can be bounded from below as

$$\begin{aligned} g_n^\omega(\lambda, h) &= \frac{1}{n} \log E \left(\exp \left[\lambda \sum_{i=1}^n (\omega_i + h)(\Delta_i - 1) \right] \right) \\ &\geq \frac{1}{n} \log E \left(\exp \left[\lambda \sum_{i=1}^n (\omega_i + h)(\Delta_i - 1) \right] 1_{\mathcal{W}_{n,l,\delta}^\omega} \right) \\ &\geq \frac{1}{n} \log \left\{ \left(\prod_{j=1}^{t_{n,l,\delta}^\omega} b(\tau_j^\omega l) b(l) e^{-2\lambda(-\delta+h)l} \right) a(n - i_{t_{n,l,\delta}^\omega}^\omega l) \right\} \\ &\geq \frac{1}{n} \sum_{j=1}^{t_{n,l,\delta}^\omega} \log b(\tau_j^\omega l) + \frac{t_{n,l,\delta}^\omega}{n} [\log b(l) + 2\lambda(\delta - h)l] + \frac{1}{n} \log a(n), \end{aligned} \quad (9.34)$$

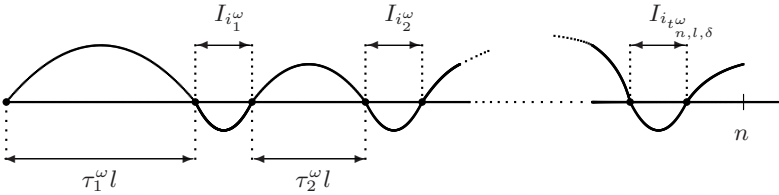


Fig. 9.5. A path in $\mathcal{W}_{n,l,\delta}^\omega$.

where $a(k)$ and $b(k)$ are defined in (9.13), the second inequality uses that $\Omega_j \leq -\delta l$ for $j = 1, \dots, t_{n,l,\delta}^\omega$, and the third inequality uses that $k \mapsto a(k)$ is non-increasing. We need to compute the ω -a.s. limit of the right-hand side of (9.34) as $n \rightarrow \infty$.

The last term vanishes as $n \rightarrow \infty$, because $a(n) \asymp n^{-1/2}$. Furthermore, since there exists a $C > 0$ such that $b(k) \geq Ck^{-3/2}$ for $k \in 2\mathbb{N}$, we have

$$\begin{aligned} \frac{1}{n} \sum_{j=1}^{t_{n,l,\delta}^\omega} \log b(\tau_j^\omega l) &\geq \frac{1}{n} \sum_{j=1}^{t_{n,l,\delta}^\omega} \log \left[C(\tau_j^\omega l)^{-3/2} \right] \\ &\geq -\frac{3t_{n,l,\delta}^\omega}{2n} \log \left[\frac{\sum_{j=1}^{t_{n,l,\delta}^\omega} \tau_j^\omega l}{t_{n,l,\delta}^\omega} \right] + \frac{t_{n,l,\delta}^\omega}{n} \log C, \end{aligned} \quad (9.35)$$

where the second inequality uses Jensen's inequality. Moreover, applying the ergodic theorem to $(\Omega_j)_{j \in \mathbb{N}}$ while recalling (9.31–9.32), we have

$$\lim_{n \rightarrow \infty} \frac{t_{n,l,\delta}^\omega}{n} = p_{l,\delta} \quad \omega - a.s., \quad (9.36)$$

where

$$p_{l,\delta} = \frac{1}{l} q_{l,\delta} (1 - q_{l,\delta}) \text{ with } q_{l,\delta} = \mathbb{P}(\Omega_1 \leq -\delta l). \quad (9.37)$$

Since $\sum_{j=1}^{t_{n,l,\delta}^\omega} \tau_j^\omega l \leq n - t_{n,l,\delta}^\omega l$, it follows from (9.36) that

$$\limsup_{n \rightarrow \infty} \frac{\sum_{j=1}^{t_{n,l,\delta}^\omega} \tau_j^\omega l}{t_{n,l,\delta}^\omega} \leq \lim_{n \rightarrow \infty} \frac{n - t_{n,l,\delta}^\omega l}{t_{n,l,\delta}^\omega} = p_{l,\delta}^{-1} - l \quad \omega - a.s. \quad (9.38)$$

Combining (9.34–9.38) and recalling (9.21), we arrive at

$$g(\lambda, h) \geq -\frac{3}{2} p_{l,\delta} \log(p_{l,\delta}^{-1} - l) + p_{l,\delta} \left[2 \log C - \frac{3}{2} \log l + 2\lambda(\delta - h)l \right]. \quad (9.39)$$

This inequality is valid for all $l \in 2\mathbb{N}$ and $\delta \in (0, 1]$.

Next, let

$$\Sigma(\delta) = \sup_{\lambda > 0} [\lambda \delta - \log \mathbb{E}(e^{-\lambda \omega_1})], \quad \delta \in (0, 1], \quad (9.40)$$

denote the Legendre transform of the cumulant generating function of $-\omega_1$, where we note that, by the symmetry of the distribution of ω_1 , the supremum over $\lambda \in \mathbb{R}$ reduces to the supremum over $\lambda > 0$. Then, by Cramér's theorem of large deviation theory (see e.g. den Hollander [168], Chapter I), we have

$$\lim_{l \rightarrow \infty} \frac{1}{l} \log q_{l,\delta} = -\Sigma(\delta) \quad \forall \delta \in (0, 1]. \quad (9.41)$$

Hence, letting $l \rightarrow \infty$ in (9.39) and using (9.37), we obtain

$$\exists \delta \in (0, 1]: -\frac{3}{2}\Sigma(\delta) + 2\lambda(\delta - h) > 0 \implies g(\lambda, h) > 0. \quad (9.42)$$

Taking the inverse Legendre transform in (9.40), we have

$$\begin{aligned} \sup_{\delta \in (0, 1]} \left[\frac{4}{3}\lambda(\delta - h) - \Sigma(\delta) \right] &= -\frac{4}{3}\lambda h + \log \mathbb{E} \left(e^{-\frac{4}{3}\lambda \omega_1} \right) \\ &= -\frac{4}{3}\lambda h + \log \cosh \left(\frac{4}{3}\lambda \right), \quad \lambda > 0. \end{aligned} \quad (9.43)$$

Combining (9.42–9.43), we get

$$\left(\frac{4}{3}\lambda \right)^{-1} \log \cosh \left(\frac{4}{3}\lambda \right) > h \implies g(\lambda, h) > 0, \quad (9.44)$$

which yields the desired lower bound on $h_c(\lambda)$. \square

9.4.3 Weak Interaction Limit

The upper and lower bounds in Theorems 9.6–9.7 are sketched in Fig. 9.6. Numerical work in Caravenna, Giacomini and Gubinelli [55] indicates that $\lambda \mapsto h_c(\lambda)$ lies somewhere halfway between these bounds (see also Garel and Monthus [244]).

The following weak interaction limit is proved in Bolthausen and den Hollander [31].

Theorem 9.8. *There exists a $K_c \in (0, \infty)$ such that*

$$\lim_{\lambda \downarrow 0} \frac{1}{\lambda} h_c(\lambda) = K_c. \quad (9.45)$$

Proof. The idea behind the proof is that, as $\lambda, h \downarrow 0$, the excursions away from the interface become longer and longer (i.e., entropy gradually takes over from energy). As a result, both w and ω can be approximated by Brownian motions. In essence, (9.45) follows from the scaling property

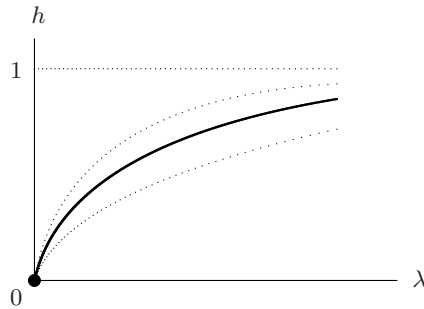


Fig. 9.6. Upper and lower bounds on $\lambda \mapsto h_c(\lambda)$.

$$\lim_{a \downarrow 0} a^{-2} f(a\lambda, ah) = \tilde{f}(\lambda, h), \quad \lambda, h \geq 0, \quad (9.46)$$

where $\tilde{f}(\lambda, h)$ is the free energy of a space-time continuous version of the copolymer model, with Hamiltonian

$$H_t^b(B) = -\lambda \int_0^t (db_s + h \, ds) \operatorname{sign}(B_s) \quad (9.47)$$

replacing (9.3), and with path measure given by the Radon-Nikodym derivative

$$\frac{dP_t^b}{dP}(B) = \frac{1}{Z_t^b} e^{-H_t^b(B)} \quad (9.48)$$

replacing (9.5). Here, $B = (B_s)_{s \geq 0}$ is a path drawn from Wiener space, replacing (9.1), P is the Wiener measure (i.e., the law of standard Brownian motion on Wiener space), and $(b_s)_{s \geq 0}$ is a standard Brownian motion, replacing (9.2), playing the role of the quenched randomness. The proof of (9.46) is based on a *coarse-graining* argument. Due to the presence of exponential weight factors, (9.46) is a much more delicate property than the standard invariance principle relating simple random walk and Brownian motion. Moreover, (9.45) follows from (9.46) only after the latter has been shown to be “stable against perturbations” in λ, h . For details we refer to [31].

In the continuum model, the quenched critical curve turns out to be *linear* with slope K_c . The value of K_c is not known. \square

The proof of (9.45) shows that the same scaling property holds for the model in which the h -dependence sits in the probability law of ω rather than in the Hamiltonian, i.e., $\mathbb{P}(\omega_i = \pm 1) = \frac{1}{2}(1 \pm h)$ and $H_n^\omega(w) = \lambda \sum_{i=1}^n \omega_i \Delta_i(w)$ instead of (9.2–9.3). This describes a copolymer where the monomers occur with different densities but interact equally strongly. Alternatively, we could allow for more general ω , assuming values in \mathbb{R} according to a symmetric distribution with a finite exponential moment (see Section 9.6). Thus, K_c has a certain degree of *universality*. See also Section 9.6, Extension (1).

The bounds in Theorems 9.6–9.7 give $K_c \in [\frac{2}{3}, 1]$. There have been various papers in the literature arguing in favor of $K_c = \frac{2}{3}$ (Stepanow, Sommer and Erukhimovich [285], Monthus [243]) and $K_c = 1$ (Trovato and Maritan [298]). Toninelli [295] proves that $K_c < 1$ (see Section 9.6, Extension (2)). The numerical work in Caravenna, Giacomin and Gubinelli [55] gives $K_c \in [0.82, 0.84]$.

9.5 Qualitative Properties of the Phases

In Section 9.5.1 we look at the path properties in the two phases, in Section 9.5.2 at the order of the phase transition, and in Section 9.5.3 at the smoothness of the free energy in the localized phase.

9.5.1 Path Properties

We next state two theorems identifying the path behavior in the two phases. The first is due to Biskup and den Hollander [20], the second to Giacomini and Toninelli [120]. These theorems confirm the naive view put forward in Section 9.3 when we defined \mathcal{L} and \mathcal{D} (recall Fig. 9.3).

Theorem 9.9. *ω -a.s. under P_n^ω as $n \rightarrow \infty$:*

- (a) *If $(\lambda, h) \in \mathcal{L}$, then the path intersects the interface with a strictly positive density, while the lengths and the heights of its excursions away from the interface are exponentially tight.*
- (b) *If $(\lambda, h) \in \text{int}(\mathcal{D})$, then the path intersects the interface with a zero density.*

Theorem 9.10. *ω -a.s. under P_n^ω as $n \rightarrow \infty$, if $(\lambda, h) \in \text{int}(\mathcal{D})$, then the path intersects the interface $O(\log n)$ times.*

The idea behind Theorem 9.9 is that in the localized regime, where the excess free energy $g = g(\lambda, h)$ defined in (9.22) is strictly positive, the probability for the copolymer to be away from the interface during a time l is roughly e^{-gl} as $l \rightarrow \infty$. This is because the copolymer contributes an amount gl to the free energy when it stays near the interface, but contributes 0 when it moves away. The idea behind Theorem 9.10 is that strictly inside the delocalized regime, where the excess free energy is zero, the probability for the copolymer to return to the interface a large number of times is small. This idea is exploited with the help of concentration inequalities.

It is believed that strictly inside the delocalized regime the number of intersections with the interface is in fact $O(1)$. This has only been proved deep inside the delocalized phase, namely, above the annealed upper bound in Theorem 9.6, where ideas similar to those that went into the proof of Theorem 7.3 can be exploited (Giacomini and Toninelli [120]). See Section 9.7, Challenge (3).

9.5.2 Order of the Phase Transition

The next theorem, due to Giacomini and Toninelli [123], shows that the phase transition is *at least* of second order.

Theorem 9.11. *For every $\lambda \in (0, \infty)$,*

$$0 \leq g(\lambda, h) = O([h_c(\lambda) - h]^2) \quad \text{as } h \uparrow h_c(\lambda). \quad (9.49)$$

Proof. We give the proof for the case where $\omega = (\omega_i)_{i \in \mathbb{N}}$ is an i.i.d. sequence of standard normal random variables, rather than binary random variables as in (9.2). At the end of the proof we indicate how to adapt the argument.

Recall the definitions in the proof of Theorem 9.7. Consider the set of paths (see Fig. 9.7)

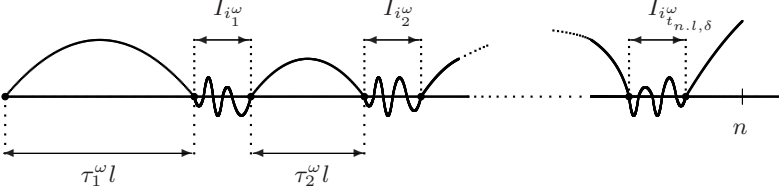


Fig. 9.7. A path in $\widehat{\mathcal{W}}_{n,l,\delta}^\omega$.

$$\widehat{\mathcal{W}}_{n,l,\delta}^\omega = \left\{ w \in \mathcal{W}_n : w_i = 0 \text{ for } i \in \bigcup_{j=1}^{t_{n,l,\delta}^\omega} \partial I_{i_j}^\omega, \right. \\ \left. w_i \geq 0 \text{ for } i \in \{(0, n] \cap \mathbb{N}\} \setminus \bigcup_{j=1}^{t_{n,l,\delta}^\omega} I_{i_j}^\omega \right\} \quad (9.50)$$

with $\partial I_j = \{(j-1)l, jl\}$, $j \in \mathbb{N}$. By restricting the path to $\widehat{\mathcal{W}}_{n,l,\delta}^\omega$, we get

$$\widetilde{Z}_n^\omega \geq \left(\prod_{j=1}^{t_{n,l,\delta}^\omega} b(\tau_j^\omega l) \widetilde{Z}_l^{T^{i_j^\omega l} \omega} \right) a(n - i_{t_{n,l,\delta}^\omega}^\omega l), \quad (9.51)$$

where T is the left-shift acting on ω , and the tilde is used to indicate that the partition sums are taken with $\Delta_i - 1$ instead of Δ_i , as in (9.20) and (9.34). Letting $n \rightarrow \infty$, using that $k \mapsto a(k)$ is non-increasing with $\lim_{n \rightarrow \infty} \frac{1}{n} \log a(n) = 0$, and noting that the convergence in (9.21) holds in \mathbb{P} -mean as well, we obtain

$$g(\lambda, h) \geq \liminf_{n \rightarrow \infty} \frac{1}{n} \mathbb{E} \left(\sum_{j=1}^{t_{n,l,\delta}^\omega} \log b(\tau_j^\omega l) \right) + \liminf_{n \rightarrow \infty} \frac{1}{n} \mathbb{E} \left(\sum_{j=1}^{t_{n,l,\delta}^\omega} \log \widetilde{Z}_l^{T^{i_j^\omega l} \omega} \right). \quad (9.52)$$

The first term in the right-hand side of (9.52) was computed in (9.35–9.38) and equals $-\frac{3}{2} p_{l,\delta} \log(p_{l,\delta}^{-1} - l)$. The expectation under the limit in the second term equals (recall (9.31–9.32))

$$\frac{1}{n} \mathbb{E} \left(\sum_{j=1}^{t_{n,l,\delta}^\omega} \log \widetilde{Z}_l^{T^{i_j^\omega l} \omega} \right) = \mathbb{E} \left(\frac{t_{n,l,\delta}^\omega}{n} \right) \mathbb{E} \left(\log \widetilde{Z}_l^\omega \mid \Omega_1 \leq -\delta l \right). \quad (9.53)$$

Conditioning l i.i.d. normal random variables with mean 0 and variance 1 to have sum equal to $-\delta l$ is the same as taking l i.i.d. normal random variables with mean $-\delta$ and variance 1. Hence, the effect of the conditioning in (9.53) is that, in (9.20), ω_i becomes $\omega_i - \delta$, so that

$$\mathbb{E}(\log \widetilde{Z}_l^\omega(\lambda, h) \mid \Omega_1 \leq -\delta l) = \mathbb{E}(\log \widetilde{Z}_l^\omega(\lambda, h - \delta)), \quad (9.54)$$

where we add the parameters λ, h as arguments to exhibit the shift in h . Inserting (9.54) into (9.53), picking $h = h_c(\lambda)$ in (9.52), noting that $g(\lambda, h_c(\lambda)) = 0$, and recalling (9.36), we arrive at

$$0 \geq -\frac{3}{2} p_{l,\delta} \log(p_{l,\delta}^{-1} - l) + p_{l,\delta} \mathbb{E}(\log \tilde{Z}_l^\omega(\lambda, h_c(\lambda) - \delta)). \quad (9.55)$$

This inequality is valid for all $l \in 2\mathbb{N}$ and $\delta \in (0, 1]$.

Dividing (9.55) by l , letting $l \rightarrow \infty$ and using (9.41), we obtain

$$0 \geq -\frac{3}{2} \Sigma(\delta) + g(\lambda, h_c(\lambda) - \delta), \quad (9.56)$$

where Σ is the Cramér rate function for standard normal random variables, i.e., $\Sigma(\delta) = \frac{1}{2}\delta^2$. Hence we conclude that

$$g(\lambda, h_c(\lambda) - \delta) \leq \frac{3}{4}\delta^2, \quad (9.57)$$

which proves the claim.

It is easy to extend the proof to binary ω . All that is needed is to show that (9.54) holds asymptotically as $l \rightarrow \infty$ and to use that $\Sigma(\delta) \sim \frac{1}{2}\delta^2$ as $\delta \downarrow 0$. \square

9.5.3 Smoothness of the Free Energy in the Localized Phase

We conclude with a theorem by Giacomin and Toninelli [124] showing that the free energy is smooth throughout the localized phase. Consequently, our critical curve is the *only* location where a phase transition of *finite order* occurs.

Theorem 9.12. $(\lambda, h) \mapsto f(\lambda, h)$ is infinitely differentiable on \mathcal{L} .

Proof. The main idea behind the proof is that, for $(\lambda, h) \in \mathcal{L}$, the correlation between any pair of events that depend on the values of the path w of the copolymer in finite and disjoint subsets of $\{1, \dots, n\}$ decays exponentially with the distance between these sets. This is formulated in the following lemma.

Lemma 9.13. Let \mathcal{K} be an arbitrary compact subset of \mathcal{L} . Then there exist $0 < c_1, c_2 < \infty$ (depending on \mathcal{K}) such that, for all $(\lambda, h) \in \mathcal{K}$, all $n \in \mathbb{N}$, all integers $1 \leq a_1 < b_1 < a_2 < b_2 \leq n$, and all pairs of events A and B that are measurable w.r.t. the sigma-fields generated by $(w_{a_1}, \dots, w_{b_1})$, respectively, $(w_{a_2}, \dots, w_{b_2})$,

$$\mathbb{E}(|P_n^\omega(A \cap B) - P_n^\omega(A) P_n^\omega(B)|) \leq c_1 e^{-c_2(a_2 - b_1)}. \quad (9.58)$$

Proof. The proof of Lemma 9.13 is based on the following lemma. For $n \in \mathbb{N}$, let $P_n^{\omega, \otimes 2}$ be the joint law of two independent copies w^1 and w^2 of w of length n .

Lemma 9.14. There exist $0 < c_1, c_2 < \infty$ (depending on \mathcal{K}) such that for all $(\lambda, h) \in \mathcal{K}$, all $n \in \mathbb{N}$, and all integers $1 \leq a < b \leq n$,

$$\mathbb{E}(P_n^{\omega, \otimes 2}(E_{a,b})) \leq c_1 e^{-c_2(b-a)}, \quad (9.59)$$

where $E_{a,b} = \{\#i \in \{a+1, \dots, b-1\} : w_i^1 = w_i^2 = 0\}$.

Proof. The main idea is that, for $(\lambda, h) \in \mathcal{L}$, the lengths of the excursions of the copolymer away from the interface are exponentially tight. This forces w^1 and w^2 to hit the interface in a set of sites with a strictly positive density. Therefore the probability that w^1 and w^2 hit the interface at the same site at least once in $\{a+1, \dots, b-1\}$ tends to 1 exponentially fast as $b-a \rightarrow \infty$. For details we refer the reader to Giacomin and Toninelli [124]. \square

Now note that the l.h.s. of (9.58) is equal to

$$\mathbb{E} \left(\left| E_n^{\omega, \otimes 2} [\{1_A(w^1)1_B(w^1) - 1_A(w^1)1_B(w^2)\} 1_E(w^1, w^2)] \right| \right). \quad (9.60)$$

Together with (9.59), this completes the proof of Lemma 9.13. \square

We use Lemma 9.13 to complete the proof of Theorem 9.12. This can be done by appealing to the theorem of Arzela-Ascoli, according to which it is enough to prove that for every $k_1, k_2 \in \mathbb{N}$ the partial derivative

$$\frac{\partial^{k_1+k_2}}{\partial \lambda^{k_1} \partial h^{k_2}} \left(\frac{1}{n} \mathbb{E} \log Z_n^\omega \right) \quad (9.61)$$

is bounded from above, uniformly in $n \in \mathbb{N}$ and $(\lambda, h) \in \mathcal{K}$.

In order to achieve the latter, we define, for $k \in \mathbb{N}$ and for $\{f_1, \dots, f_k\}$ any family of bounded functions on the path space \mathcal{W}_n whose supports are finite,

$$E_n^\omega[f_1(w); \dots; f_k(w)] = \sum_{P \in \mathcal{P}} (-1)^{|P|-1} (|P|-1)! \prod_{p=1}^{|P|} E_n^\omega \left[\prod_{l \in P_p} f_l(w) \right], \quad (9.62)$$

where \mathcal{P} denotes the set of all partitions $P = (P_p)_{p \in |P|}$ of $\{1, \dots, k\}$, with $|P|$ the number of sets in the partition P . We need the following lemma for this quantity.

Lemma 9.15. *For all $k \in \mathbb{N}$ there exist $0 < c_1, c_2 < \infty$ (depending on k and \mathcal{K}) such that, for all $(\lambda, h) \in \mathcal{K}$,*

$$\mathbb{E} \left[|E_n^\omega[f_1; \dots; f_k]| \right] \leq c_1 \|f_1\|_\infty \dots \|f_k\|_\infty e^{-c_2(|\mathcal{I}| - |\mathcal{S}(f_1)| + \dots + |\mathcal{S}(f_k)|)}, \quad (9.63)$$

where $\mathcal{S}(f_1), \dots, \mathcal{S}(f_k)$ are the supports of f_1, \dots, f_k , and \mathcal{I} is the smallest interval containing $\mathcal{S}(f_1), \dots, \mathcal{S}(f_k)$.

Proof. The proof uses induction on k . We skip the details, noting only that the case $k = 1$ is trivial, while the case $k = 2$ is a direct consequence of Lemma 9.13 after we write bounded functions with finite support as linear combinations of indicators of events. \square

The point of the notation introduced in (9.62) is that (9.61) can be written in the form

$$\begin{aligned} & \frac{1}{n} \sum_{1 \leq i_1, \dots, i_{k_1} \leq n} \sum_{1 \leq j_1, \dots, j_{k_2} \leq n} \mathbb{E} \left[(\omega_{i_1} + h) \dots (\omega_{i_{k_1}} + h) \right. \\ & \quad \left. \times E_n^\omega [\Delta_{i_1}(w); \dots; \Delta_{i_{k_1}}(w); \Delta_{j_1}(w); \dots; \Delta_{j_{k_2}}(w)] \right]. \end{aligned} \quad (9.64)$$

Since the ω_i 's are bounded, the proof will therefore be complete once we show that

$$\frac{1}{n} \sum_{1 \leq i_1, \dots, i_k \leq n} \mathbb{E} \left[|E_n^\omega [\Delta_{i_1}(w); \dots; \Delta_{i_k}(w)]| \right], \quad k = k_1 + k_2, \quad (9.65)$$

is bounded uniformly in $n \in \mathbb{N}$ and $(\lambda, h) \in \mathcal{K}$. For this we use Lemma 9.15, to bound (9.65) from above by

$$\frac{1}{n} \sum_{m=1}^{n-1} \sum_{(i_1, \dots, i_k) \in T_n^m} c_1 e^{-c_2(m-k)}, \quad (9.66)$$

where

$$\begin{aligned} T_n^m = \{ & (i_1, \dots, i_k) : 1 \leq i_1, \dots, i_k \leq n, \\ & \max\{i_1, \dots, i_k\} - \min\{i_1, \dots, i_k\} = m \}. \end{aligned} \quad (9.67)$$

Since $|T_n^m| \leq nm^k$, (9.66) is at most $c_1 e^{c_2 k} \sum_{m \in \mathbb{N}} m^k e^{-c_2 m} < \infty$. \square

9.6 Extensions

(1) With the exception of Theorem 9.11, all the results described in Sections 9.2–9.5 extend to the situation where the ω_i are \mathbb{R} -valued with a finite moment generating function. For instance, define

$$h^*(\lambda) = \frac{1}{2\lambda} \log \mathbb{E} (e^{2\lambda\omega_1}), \quad \lambda \in (0, \infty), \quad (9.68)$$

and assume that h^* is finite on $(0, \infty)$. Then the proofs of Theorems 9.6–9.7 show that

$$h^*\left(\frac{2}{3}\lambda\right) \leq h_c(\lambda) \leq h^*(\lambda), \quad \lambda \in (0, \infty). \quad (9.69)$$

Moreover, if the random walk is replaced by a renewal process whose return times to the interface have distribution $P(S_i > 0 \forall 0 < i < n, S_n = 0) \sim n^{-1-a} L(n)$ as $n \rightarrow \infty$ for some $a > 0$ and some function L that is slowly varying at infinity (as in (7.5)), then the same proofs yield

$$h^*\left(\frac{1}{1+a}\lambda\right) \leq h_c(\lambda) \leq h^*(\lambda), \quad \lambda \in (0, \infty). \quad (9.70)$$

We refer the reader to Giacomin [116], Chapters 6–8, for a full account of these extensions. The reason why the generalization from random walks to renewal processes works is precisely that the Hamiltonian in (9.3) decomposes

into contributions coming from single excursions away from the interface. Therefore only the asymptotics of the law of these excursions matters. It also allows for the inclusion of $(1 + d)$ -dimensional excursions away from a d -dimensional flat interface with $d \geq 2$.

Theorem 9.11 has been extended to bounded disorder, and also to continuous disorder subject to a mild entropy condition that is satisfied e.g. for Gaussian disorder (see Giacomin and Toninelli [122], [123]).

(2) Toninelli [294] shows that the upper bound in Theorem 9.6 is strict for unbounded disorder and large λ . This result is extended by Bodineau, Giacomin, Lacoïn and Toninelli [23] to arbitrary disorder (subject to h^* in (9.68) being finite) and arbitrary λ . The proofs are based on *fractional moment estimates* of the partition sum. Toninelli [295] further refines the latter technique to show that $K_c < 1$ for arbitrary disorder, thereby ruling out $K_c = 1$ (recall the discussion at the end of Section 9.4.3). Bodineau, Giacomin, Lacoïn and Toninelli [23] also show that the lower bound in Theorem 9.7 is strict for arbitrary disorder and small λ , at least for a large subclass of excursion return time distributions. The proof is based on finding appropriate *localization strategies*, in the spirit of the computation in Section 9.4.2.

(3) The difficulty behind improving the upper bound is that the typical length of the excursions diverges as the critical curve is approached from below. Consequently, any attempt to do a higher order partial annealing in the hope to improve the first order partial annealing argument in (9.28) is doomed to fail. This fact was observed in Orlandini, Rechnitzer and Whittington [253] and in Iliev, Rechnitzer and Whittington [182], and was subsequently proved for a large class of models in Caravenna and Giacomin [54]. In the latter paper, the setting is an arbitrary Hamiltonian $w \mapsto H_n^\omega(w)$ with the property that there exists a sequence $(D_n)_{n \in \mathbb{N}}$ of subsets of \mathbb{Z}^d such that

$$\begin{aligned} \lim_{n \rightarrow \infty} \frac{1}{n} \log P(w_i \in D_i \ \forall 1 \leq i \leq n) &= 0, \\ w_i \in D_i \ \forall 1 \leq i \leq n &\implies H_n^\omega(w) = 0 \ \forall \omega, \end{aligned} \tag{9.71}$$

where P is the reference path measure. Given an arbitrary local, bounded and measurable function $\omega \mapsto F(\omega)$ with $\mathbb{E}(F(\omega)) = 0$, it is shown

$$\begin{aligned} \liminf_{n \rightarrow \infty} \frac{1}{n} \log \mathbb{E}(E(\exp[-H_n^\omega(S)])) &> 0 \\ \implies \liminf_{n \rightarrow \infty} \frac{1}{n} \log \mathbb{E}\left(E\left(\exp\left[-H_n^\omega(S) - \sum_{i=1}^n F(T^i \omega)\right]\right)\right) &> 0, \end{aligned} \tag{9.72}$$

where T is the left-shift acting on ω . What this says is that if the *annealed* free energy is strictly positive, then it remains strictly positive after adding the empirical average of a centered local function of the disorder. In other words, the two annealed free energies have the same critical curve. Note that the

centering implies that the *quenched* free energies associated with H and $H + F$ are the same: the term $\sum_{i=1}^n F(T^i \omega)$ does not depend on S . Thus, in order to improve an annealed estimate of a critical curve one has to resort to adding non-local functions of the disorder, which are computationally unattractive.

(4) Caravenna, Giacomini and Gubinelli [55] carry out a detailed numerical analysis of the critical curve, with full statistical control on the errors. They exploit the superadditivity property noted in the proof of Theorem 9.1, which implies that

$$g(\lambda, h) = \sup_{n \in \mathbb{N}} \frac{1}{2n} \log \mathbb{E}(\log Z_{2n}^{*, \omega}). \quad (9.73)$$

Hence, for any given (λ, h) , if $\mathbb{E}(\log Z_{2n}^{*, \omega})$ for some finite n , then $(\lambda, h) \in \mathcal{L}$. This leads to a sharp lower bound for the critical curve. It is much harder to get a decent upper bound. Computations are carried out up to $n = 2 \times 10^8$, and concentration inequalities are used to estimate the expectation \mathbb{E} with only relatively few samples of ω . Giacomini and Sohler (private communication) have pushed the computation up to $n = 10^{12}$, thereby improving the lower bound for the critical curve even further.

Interestingly, the results show that to a remarkable degree of accuracy

$$h_c(\lambda) \approx h^*(K_c \lambda), \quad \lambda \in (0, \infty), \quad (9.74)$$

with K_c the constant in (9.45), both for binary and standard normal disorder. Nevertheless, Bodineau, Giacomini, Lacoïn and Toninelli [23] prove that equality in (9.74) cannot hold for all λ , by showing that the critical curve depends on the fine details of the excursion return time distribution and not only on the universal constant K_c .

(5) The restriction to the quadrant in (9.4) can be trivially removed. Indeed, because $f(\lambda, h)$ is antisymmetric under the transformations $\lambda \rightarrow -\lambda$ and $h \rightarrow -h$ (recall (9.2–9.3)), the full phase diagram consists of four critical curves, one in each quadrant of \mathbb{R}^2 , which are images of the critical curve in the first quadrant (drawn in Fig. 9.4) under reflection in the horizontal and the vertical axes. For instance, below the critical curve in the fourth quadrant (i.e., for $h \leq -h_c(\lambda)$ and $\lambda \geq 0$) the copolymer is delocalized into the water rather than into the oil.

A further observation is the following. By subtracting $\lambda n + \lambda h \sum_{i=1}^n \omega_i$ from the Hamiltonian H_n^ω in (9.3), we obtain a new Hamiltonian

$$\widehat{H}_n^\omega(w) = -2\lambda(1+h) \sum_{i=1}^n \frac{1+\omega_i}{2} \frac{1+\Delta_i}{2} - 2\lambda(1-h) \sum_{i=1}^n \frac{1-\omega_i}{2} \frac{1-\Delta_i}{2}, \quad (9.75)$$

where we recall (9.7). In terms of the reparameterization $\alpha = 2\lambda(1+h)$ and $\beta = 2\lambda(1-h)$, this reads

$$\widehat{H}_n^\omega(w) = -\alpha \sum_{i=1}^n 1_{\{\omega_i = \Delta_i = 1\}} - \beta \sum_{i=1}^n 1_{\{\omega_i = \Delta_i = -1\}}, \quad (9.76)$$

in which energy $-\alpha$ is assigned to the hydrophobic monomers in the oil, $-\beta$ to the hydrophilic monomers in the water, and 0 to the other two combinations. By the strong law of large numbers for ω , we have $H_n^\omega - \widehat{H}_n^\omega = \lambda n + o(n)$ ω -a.s. Therefore the quenched free energies associated with H_n^ω and \widehat{H}_n^ω differ by a term $\log \lambda$, which allows for a direct link between the respective phase diagrams. The form in (9.76) is used in a number of papers (see Extensions (7–10) below), and also in Chapter 10, where we look at a copolymer near a random selective interface.

In the (α, β) -model the quenched critical curve $\alpha \mapsto \beta_c(\alpha)$ takes the form in Fig. 9.8. This curve is continuous, strictly increasing and concave as a function of α , with a finite asymptote as $\alpha \rightarrow \infty$, and with a curvature as $\alpha \downarrow 0$ that tends to K_c , the universal constant in Theorem 9.8. The former comes from the bound $1 - h_c(\lambda) \leq C/\lambda$, $\lambda \rightarrow \infty$, $C < \infty$, implied by Theorem 9.7. The latter comes from the observation that, by (9.45), as $\lambda, \alpha \downarrow 0$,

$$\alpha - \beta_c(\alpha) = 4\lambda h_c(\lambda) \sim 4K_c\lambda^2 = \frac{1}{4}K_c(\alpha + \beta_c(\alpha))^2 \sim \frac{1}{4}K_c(2\alpha)^2 = K_c\alpha^2. \quad (9.77)$$

(6) Bolthausen and Giacomin [29] look at the version of the model where the disorder is *periodic* (earlier work can be found in Grosberg, Izrailev and Nechaev [133]). For this case the free energy can be expressed in terms of a variational formula. However, it turns out to be delicate to deal with large periods, since computations quickly become prohibitive. In particular, the fact that random disorder arises from periodic disorder as the period tends to infinity seems hard to implement when probing the fine details of the critical curve. Caravenna, Giacomin and Zambotti [57], [58] look at the path properties for periodic disorder, showing that under the law P_∞^ω , i.e., the weak limit

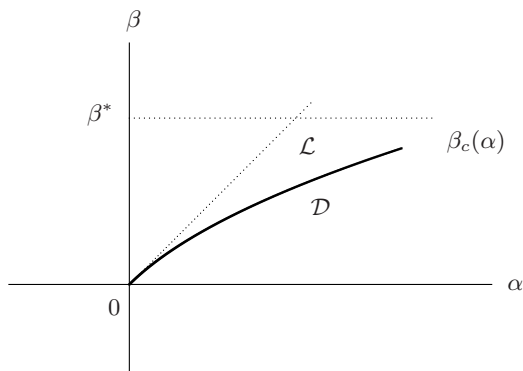


Fig. 9.8. Plot of $\alpha \mapsto \beta_c(\alpha)$.

of the law P_n^ω , the path is transient in the interior of \mathcal{D} , null-recurrent at the boundary $\partial\mathcal{D}$, and positive recurrent in \mathcal{L} . In each of the three cases they identify the scaling limit of the path.

(7) Den Hollander and Wüthrich [173] consider a version of the copolymer model with an *infinite array* of linear interfaces stacked on top of each other, equally spaced at distance L_n with n the length of the copolymer. If $\lim_{n \rightarrow \infty} L_n = \infty$, then this model has the same free energy as the single interface model, because the copolymer “sees only one interface at a time”. Under the assumption that $\lim_{n \rightarrow \infty} L_n / \log n = 0$ and $\lim_{n \rightarrow \infty} L_n / \log \log n = \infty$, they show that the copolymer hops between neighboring interfaces on a time scale of order $\exp[\chi L_n]$, for some $\chi = \chi(\lambda, h) > 0$, when $(\lambda, h) \in \mathcal{L}$. The reason is that in the localized phase the excursions away from the interface are exponentially unlikely in their length and height (recall Theorem 9.9(a)). See also Extension (7) in Section 7.6.

(8) Martin, Causo and Whittington [236] consider a version of the single interface model in which the path is self-avoiding, the sites (rather than the edges) in the path represent the monomers, while the Hamiltonian is given by (9.76). They identify the qualitative properties of the phase diagram in the (α, β) -plane with the help of exact enumeration methods, series analysis techniques and rigorous bounds. It turns out that there are two critical curves (which are images of each other w.r.t. the line $\{\alpha = \beta\}$ when both monomer types occur with density $\frac{1}{2}$). Both curves lie in the first and in the third quadrant, with horizontal and vertical asymptotes, and meet each other at the origin. Below the lower curve the copolymer is delocalized into the water, above the upper curve it is delocalized into the oil, while in between the two curves it is localized near the interface. Madras and Whittington [233], building on earlier work by Maritan, Riva and Trovato [235], prove that inside the first quadrant the lower curve lies strictly inside the first octant except at the origin, and is a continuous, non-decreasing and concave function of α (and thus is similar to the one in Fig. 9.8, showing that the SAW-restriction does not alter the qualitative properties of the phase diagram). Causo and Whittington [64] analyze the phase diagram with the help of Monte Carlo techniques, and their results suggest that the phase transition is second order in the third quadrant but higher order in the first quadrant. If the latter were true, then this would imply that the origin is a tricritical point, i.e., a point where three phases meet. The results in [235], [236] and [233] apply to SAW's in dimensions $d \geq 2$.

(9) James, Soteris and Whittington [198], [199] generalize the SAW-version of the (α, β) -model by adding to the Hamiltonian an energy $-\gamma$ for each monomer that lies at the interface, irrespective of its type. It turns out that the value of γ affects the phase diagram (see Fig. 9.9). Indeed, as later shown in Madras and Whittington [233], for $\gamma < 0$ the phase diagram is qualitatively like that for $\gamma = 0$, but not for $\gamma > 0$. Indeed, there are *two critical values* $0 \leq \gamma_1 \leq \gamma_2 < \infty$ such that for $\gamma \in (\gamma_1, \gamma_2)$ the two critical curves are separated,

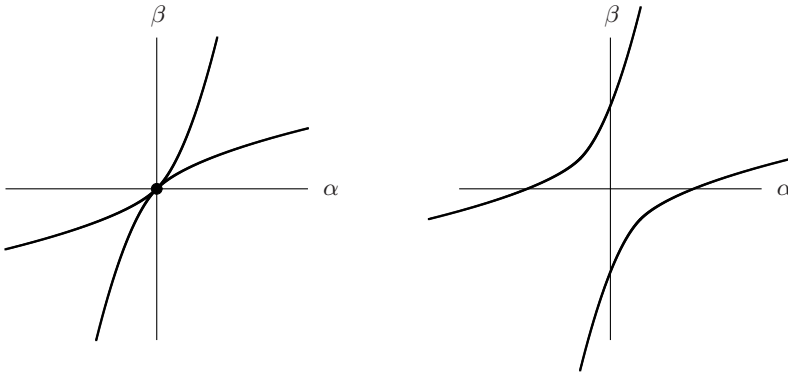


Fig. 9.9. Phase diagrams for the (α, β, γ) -model. The first curve is for $\gamma \in (-\infty, \gamma_1]$, the second curve for $\gamma \in (\gamma_1, \gamma_2)$. For $\gamma \in [\gamma_2, \infty)$ both curves have moved out to infinity.

i.e., they pass through the second and the fourth quadrant (resulting in a single localized phase), while for $\gamma \in [\gamma_2, \infty)$ the two critical curves have “moved out to infinity”, i.e., the system is localized for all values of (α, λ) . It is shown that $\gamma_2 < \infty$. It is believed that $\gamma_1 = 0$ and $\gamma_2 > 0$, but this remains open. For $\alpha = \beta = 0$ the model reduces to the homogeneous pinning model described in Section 7.1. Also the results in [198] and [199] apply to SAW’s in dimensions $d \geq 2$. Exact enumeration is done for $d = 3$.

Habibzadah, Iliev, Saguia and Whittington [140] analyze the (α, β, γ) -model for generalized ballot paths rather than ballot paths (recall Fig. 1.4). The qualitative properties of the phase diagram are the same as for self-avoiding paths.

(10) Iliev, Orlandini and Whittington [181] study the effect of a force in the (α, β) -model with $\alpha < 0$ and $\beta > 0$, i.e., when the copolymer is delocalized below the interface. The force is applied to the endpoint of the copolymer and is perpendicular to the interface in the upward direction (in the spirit of the models considered in Section 7.3). Both for ballot paths and for generalized ballot paths the quenched free energy is computed in the first order Morita approximation, i.e., Z_n^ω is averaged over ω conditioned on $n^{-1} \sum_{i=1}^n \omega_i = 0$. Even though the Morita free energy is only an upper bound for the quenched free energy, it is argued that both free energies lead to the same critical force, which can therefore be computed explicitly. The critical curve in the force-temperature diagram is strictly increasing and so the phase transition is *not re-entrant* (compare with Section 7.3).

The situation is different when $\beta \geq \alpha > 0$. In that case the phase transition is *re-entrant* for $\beta > \alpha$, with the critical curve in the force-temperature diagram hitting 0 at some finite temperature, and *not re-entrant* for $\beta = \alpha$, with the critical curve being strictly increasing. This fits with the observations made

in Extension (4), where the critical curve in the phase diagram of the (α, β) -plane without force was found to touch the line $\{\alpha = \beta\}$ (see Fig. 9.8). It is argued that the critical curve in the force-temperature diagram in the Morita approximation is an upper bound for the one of the quenched model.

(11) For the directed version of the (α, β, γ) -model, Orlandini, Tesi and Whittington [254] and Orlandini, Rechnitzer and Whittington [253] analyze the phase diagram in the Morita approximation, i.e., they compute the annealed free energy subject to restrictions on the first and second moments of ω . This gives only limited rigorous information on the properties of the critical curves, but it provides considerable insight into the mechanisms driving the phase transition. The analysis was subsequently extended by Iliev, Rechnitzer and Whittington [182], who found evidence that the lower critical curve is non-analytic at the origin when $\gamma = 0$, at a point in the third quadrant when $\gamma < 0$, and at a point in the first quadrant when $\gamma > 0$. The nature of these tricritical points remains unclear.

(12) Brazhnyi and Stepanow [40] consider a model of a random copolymer in \mathbb{R}^3 where the Hamiltonian includes elasticity, self-repulsion and self-attraction, thereby combining aspects from Chapters 3–6 and 9. Obviously, such models display highly complex behavior, but they are worthwhile to investigate when the aim is to model particular experimental situations. With a combination of analytical and numerical techniques it is shown that localization is disfavored by self-repulsion, favored by self-attraction, and can be re-entrant as a function of the densities of the different monomer types.

9.7 Challenges

(1) Improve Theorem 9.11 by finding out whether the phase transition is second order or higher order. Numerical analysis seems to indicate that the order is higher (Trovato and Maritan [298], Causo and Whittington [64], Caravenna, Giacomini and Gubinelli [55]). Monthus [243] suggests that the order is infinite.

(2) We know from Theorem 9.12 that the quenched free energy is infinitely differentiable on \mathcal{L} . Find out whether or not it is analytic. At points where this fails the system is said to have a Griffiths-McCoy singularity (Griffiths [132], McCoy [239]). Such singularities are known to occur in some disordered systems, e.g. the low-temperature dilute Ising model in zero magnetic field. The singular behavior is due to the occurrence of rare but arbitrarily large regions where the disorder is such that locally the system is almost at a phase transition. Is the critical curve, i.e., the boundary of \mathcal{L} , analytic?

(3) Improve Theorem 9.10 by showing that the path intersects the interface only finitely often. This has been proved by Giacomini and Toninelli [120] deep inside \mathcal{D} , namely, for (λ, h) on or above the annealed critical curve that is the upper bound in Theorem 9.6.

- (4) Identify the analogue of the weak interaction limit in (9.46–9.48) when the reference random walk is not SRW (see Section 9.6, Extension (1)).
- (5) The global properties of the copolymer do not depend on the fact that the monomer types are drawn in an i.i.d. rather than a stationary ergodic fashion, but the local properties do. Since in real polymers the order of the monomer types is at best Markov (as a result of the underlying polymerization process), it is interesting to try and extend the results in Sections 9.2–9.5 to the Markov setting.
- (6) Investigate whether or not the critical curve for the SAW-version of the (α, β) -model defined in Section 9.6, Extension (8), has a positive and finite curvature as $\alpha \downarrow 0$. Is this curvature equal to K_c , as in the directed version of the (α, β) -model, or not? Prove that $\gamma_1 = 0$ in the SAW-version of the (α, β, γ) -model defined in Section 9.6, Extension (9).